Multi-Disciplinary Senior Design Conference
Kate Gleason College of Engineering
Rochester Institute of Technology
Rochester, New York 14623

**Project Number: P08441**

# P08441: THERMOELECTRIC AUTO EXHAUST POWER GENERATION TECHNICAL PAPER

**Stephen Byrne-ME**
**Frank Trotto-EE**
**Erin Crowley-ME**
**Paul Gaylo-ME**
**Mike Rheinheimer-ME**
**Joel Nelson-EE**

## ABSTRACT

Project P08441, Automotive Exhaust Power Generation Unit, is a six month design project focused on gaining experience in the performance and operating characteristics of contemporary thermoelectric modules. The specific avenue of investigation is centered on the electric response of an array of modules when exposed to a typical automotive exhaust stream and the temperature gradient associated with that stream. A precise thermal model, an item of special attention from this project, illustrates the theoretical performance of the prototype test fixture. While current technology does not allow for efficient or economical implementation of a thermoelectric device in production, it is anticipated that technologies on the horizon will facilitate the integration of thermoelectrics as an energy reclamation scheme. This project has operated on the premise that a better understanding of the run-characteristics of current commercial thermoelectric offerings will be a first step to the integration of future thermoelectric technologies.

## NOMENCLATURE

$\alpha \Rightarrow$ Thermal Expansion Coefficient
$\alpha_m \Rightarrow$ Seebeck Coefficient
$D_H \Rightarrow$ Hydraulic Diameter
$f \Rightarrow$ Friction Factor
$h \Rightarrow$ Convective Coefficient
I $\Rightarrow$ Electrical Current (Amps)
$I_z \Rightarrow$ Moment of Inertia
$k \Rightarrow$ Thermal Conductivity
$k_b \Rightarrow$ Bolt Stiffness
$k_m \Rightarrow$ Member Stiffness
$m \Rightarrow$ Meter
$m_{DOT} \Rightarrow$ Mass Flow Rate
$Nu_D \Rightarrow$ Nusselt Number
$\rho \Rightarrow$ Density
$\Delta P \Rightarrow$ Pressure Difference
$q_c \Rightarrow$ Heat Flow into Cold Side
$q_h \Rightarrow$ Heat Flow into Hot Side
$R \Rightarrow$ Resistance
$T_1 \Rightarrow$ Temperature of TEG, hot side
$T_2 \Rightarrow$ Temperature of TEG, cold side
$T_{h,i} \Rightarrow$ Temperature of Exhast Entering
$T_{h,i+1} \Rightarrow$ Temperature of Exhaust Leaving
$v \Rightarrow$ Velocity
$V \Rightarrow$ Voltage
$W \Rightarrow$ Watts

# I) INTRODUCTION

### Project Background

The motivation for this project stems from an increasing need for highly efficient power generation in the transportation sector. Thermoelectric power generation is seen as a possible step in gathering efficiency in an economical manner, Furthermore, motivation lies in the general understanding of the operation and feasibility of thermoelectric power recovery. P08441 will build upon two previous senior design projects by implementing integral testing equipment which has already been designed.

Thermoelectrics, as heating or cooling devices, are not a new in concept, but when viewed from a power generation stance, the field is still young and evolving. The basic operation of a thermoelectric as a power generating devices stems around the need for a large temperature difference across the module. Creating a large temperature differential allows the module to produce more power by way of the thermoelectric effect which is based on the Peltier and Seebeck effect [1]. Thermoelectrics use p and n-type semiconductors connected in series and create a voltage proportional to the temperature gradient across the thermoelectric [2].

# II) PROCESS

### Project Needs

In conjunction with, Dr. Robert Stevens, the customer and guide of project P08441, the project needs were developed. The project needs fuel and direct the design process. Specifically, for this project, thermoelectric power generation, heat transfer, testing and design verification, safety, and durability all tie into the specific needs.

### Project Engineering Specifications

Customer Needs and Engineering Specifications tabulated below are the key engineering specifications that are to be met. The specifications directly govern the design decisions made and the type of engineering analysis performed. All specifications shall be verified on the thermoelectric test stand created by project P07442, a previous senior design team. The test conditions, which were based on real world data supplied by the Delphi Corporation identifying the exhaust characteristics of a typical 4 cylinder engine. The test conditions are as follows:

| Mass Flow Rate | Exhaust Temperature | Room Temperature | Blower Air Velocity |
|---|---|---|---|
| kg/s | K | K | m/s |
| 0.04 | 550 | 295-300 | 17.1 |

**Table 1. Engineering Specs.**

The test conditions were used in the thermal and fluid analysis performed for this project.

| Specification | Units | Ideal Value |
|---|---|---|
| Adequate power generation | W | 100+ (65 marginal) |
| Output voltage adequate to charge battery | V | 14 |
| Design must stay within budget | $ | 3000 |
| Overall system efficiency increase | % | 1 |
| Hot side of TEG at proper temperature | °C | 225 |
| Cold side of TEG at proper temperature | °C | 100 |
| Pressure drop across unit | Pa | 1100 |

**Table 2- Key Engineering Specifications**

Cost benefit analysis was performed on various types of thermoelectric modules, including models for Hi-Z, Tellurex, and Melcor. Ultimately, the analysis showed that the Melcor units would be the most cost effective option. Therefore, all the system modeling is based upon using the Melcor HT8-12-40 thermoelectric modules.

### Concept Analysis & Evaluation

As explained earlier a thermoelectric generator functions on the Seebeck effect – that electrical power can be produced in a temperature gradient. A portion of the heat flow entering one side of the thermoelectric is converted to electrical power. On the other side of the device, the heat flow leaves, minus the fraction that was converted. Thermoelectric modules, as they stand today, are only around 2-5% efficient. As a result, heat transfer analysis is critical in ensuring that enough heat flows through the for them to be modules effective.

The system of equations that relates the heat transfer to the electrical current produced from a single module is as follows:

$$q_{h,i} = \frac{T_{A,i} - T_{B,i}}{R_{th,TE}} - \frac{1}{2} I^2 R_{e,TE} + \alpha_m T_{A,i} I + \frac{T_{A,i} - T_{B,i}}{R_{th,ins}}$$

$$q_{c,i} = \frac{T_{A,i} - T_{B,i}}{R_{th,TE}} + \frac{1}{2} I^2 R_{e,TE} + \alpha_m T_{B,i} I + \frac{T_{A,i} - T_{B,i}}{R_{th,ins}}$$

$$I = \frac{\alpha_m (T_{A,i} - T_{B,i})}{R_{e,TE} + R_{e,L}}$$

$$T_{A,i} = \frac{T_{h,i} + T_{h,i+1}}{2} - q_{h,i} R_{th,H}$$

$$T_{B,i} = q_c R_{th,C} + T_C$$

$$T_{h,i} = \frac{R_{th,TE} m_{dot} c_{p,h} T_{h,i} - T_{A,i} + T_{B,i} + \frac{1}{2} I^2 R_{e,TE} R_{th,TE} - \alpha_m T_{A,i} I R_{th,TE}}{R_{th,TE} m_{dot} c_{p,h}}$$

**Equation 1: System of Equations**

The system of equations detailed in equation 1. includes the Seebeck coefficient. The system of equations is able to calculate the heat flow through an individual thermoelectric module based on the thermoelectric's thermal and electrical resistance, hot side thermal resistance, cold side thermal resistance, and the input exhaust characteristics. Since the TEG unit is removing heat from the exhaust gas the parameters change for downstream thermoelectrics. To find the total current output of a given TEG configuration, the equations must be set up in an iterative format to take into consideration the heat being removed from the system. Microsoft Excel was used to create the model and perform the iterative calculations.

The assumptions made for this model include negligible heat transfer through insulation surrounding TEG modules, a load resistance on each TEG equal to the electrical resistance of a TEG, fully developed turbulent flow, uniform convection, negligible radiation effects, one-dimensional heat conduction, and uniform flow through each channel in heat exchanger. The exhaust parameters were decided upon based on average car exhaust conditions. The mass flow rate was taken as .04 *kg/s* at a temperature of 280°C.

To maximize heat flow through the thermoelectrics an attempt was made to keep the thermal and contact resistances of all of the materials in the thermal circuit minimized. In addition, the pressure drop associated with obstructions in the exhaust flow was taken into account. The following relations were used in finding the thermal resistance in the heat exchanger **[3].**

$$\mathrm{Re} = \frac{\frac{m_{dot}}{A_{channels}} D_h}{\mu} = \frac{\frac{0.04 kg/s}{0.00398 \mathrm{m}^2} \times 0.00893 \mathrm{m}}{2.97 \times 10^{-5} Ns/m^2} = 48300$$

**Equation 2. Reynolds Number**

$$f = 0.184 \,\mathrm{Re}_D^{-1/5} \text{ for } \mathrm{Re}_D \geq 2 \times 10^4$$

$$f = .0213$$

**Equation 3. Friction Factor**

$$Nu_D = \frac{(f/8)(\mathrm{Re}_D - 1000)\,\mathrm{Pr}}{1 + 12.7(f/8)^{1/2}(\mathrm{Pr}^{2/3} - 1)} = 146$$

$$h = Nu_D \frac{k}{D_h} = 854 \,\mathrm{W/m^2 - K}$$

**Equation 4. Nusselt Number**

For interfaces where thermal paste or thermal adhesive was used, the contact resistance was taken to be that associated with the conductivity of the material used.

**Total Fin Thermal Resistance (one TE) = 0.33 *K/W* *(hot side)***

Manufacturer's data was used along with calculated contact resistances to determine the total external thermal resistance. The heat sinks were purchased from Aavid Thermalloy. The chart shown below was used to find the thermal resistance. The desired air speed was around 17 *m/s* and, as shown in the chart below (Figure 4), manufacturer's data did not give values for air speed above 6 *m/s*. A technical representative was contacted and recommended a linear extrapolation of the data.

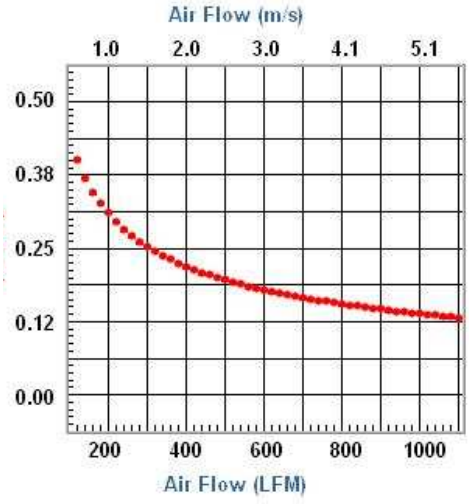


**Figure 4. Aavid Thermalloy Air Flow Graph**

**Total Fin Thermal Resistance (one TE) = 0.23 *K/W* *(cold side)***

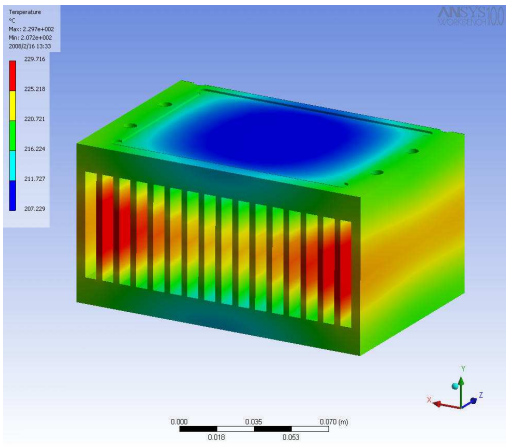

**Figure 5: Thermal Model**

The finite element software, ANSYS 10.0, was implemented to verify the analytical thermal model for the first row the thermoelectric modules. The input parameters used for the exhaust characteristics were based on the standard test conditions. The resulting hot side temperature of the thermoelectrics came out to roughly 209°C.

**Pressure Drop**

The overall pressure drop throughout the TEG needs to be taken into consideration. The pressure drop is directly related to the number of internal fins in the exhaust gas stream. As the number of internal fins increases the pressure drop increases due the additional fluid friction associated with the surface area of the fins.

To model the pressure drop across the TEG the Bernoulli equation was implemented, taking into account both the major and minor head losses. The airflow was determined to be turbulent from a Reynolds number calculation. The Reynolds number was greater than 2300 at 48,300, making it turbulent. Furthermore, the expansion and contraction coefficients, for the transitions, were found on a table. Therefore, the governing equation for the pressure drop through the TEG is:

$$\mathrm{Re} = \frac{\rho v D_H}{\mu}$$

**Equation 5: Reynolds Number**

$$\Delta P = \rho \left[ f \frac{L V^2_{structure}}{2 D_{structure}} + \sum K \frac{V^2_{tube}}{2} \right]$$

**Equation 6: Change in Pressure Drop**

Where the friction factor, f, is related to the hydraulic diameter and surface finish of the internal channels. The friction factor is found on the Moody diagram [4].

With the thermal and fluid model intact it was possible to evaluate heat transfer versus pressure drop with various internal fin configurations. Finding balance between the two was integral to the concept selection and ultimate design. The analysis for both the thermal and fluid performance was based on the Standard Test Conditions. The design decisions were based on an internal fin configuration that supplied enough heat to the hot side to produce a temperature of 200°C while limiting the pressure drop as much as possible (ideally below 500 Pa).

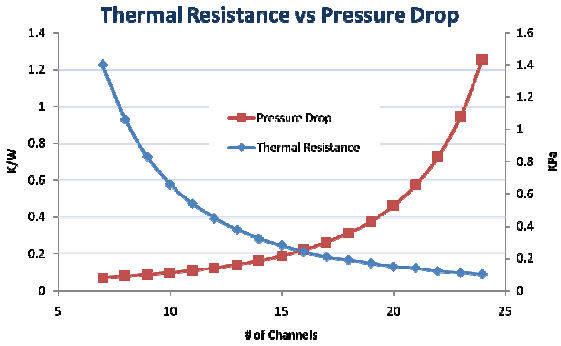


**Figure 6. Thermal Resistance vs Pressure Drop**

Analysis showed that an internal fin configuration consisting of sixteen channels provided both sufficient heat transfers while limiting the pressure drop to a minimal level. Furthermore, the model calculated that there needed to be a total of 48 thermoelectric modules, 24 to each side, to produce 100 Watts of power under the standard test conditions.

**Mechanical Calculations**

The thermoelectric manufacturer, Melcor, specifies applying a 150-300psi contact pressure to the thermoelectrics when in operation [1]. This type of pressure would require high tensile loading in the bolts holding the heat sink down. Furthermore, the heat sink itself could experience some bending, which could create stress concentrations on the edges of the brittle thermoelectric modules. Therefore, analysis was performed on both the heat sink bending and bolt strength. First, the calculations for bolt strength loading the heat sink at 300psi are as follows:

$$C = \frac{k_b}{k_b + k_m}$$

**Equation 7: Stiffness Ratio**

$$k_b = \frac{A_d A_t E}{A_d l_t + A_t l_d}$$

**Equation 8: Spring Constant (Bolt)**

$$k_m = AEde^{\left(\frac{Bd}{l}\right)}$$

**Equation 9: Spring Constant Member**

Where the factor of safety was calculated with:

$$n = \frac{S_p A_t - F_i}{CP}$$

**Equation 10: Factor of Safety**

The resulting factor of safety for 10 (on each side) 5/16"-18 Black Oxide bolts was 3.75, where the calculations were performed at the upper limit of the thermoelectric specifications [5].

In addition, the bending experienced by the heat sinks was calculated with the following equations

$$Y_{\max} = \frac{F_{TE} a}{24EI}\left(4a^2 - 3l^2\right)$$

**Equation 11: Deflection**

$$I_z = \frac{m}{12}\left(b^2 + c^2\right)$$

**Equation 12: Moment of Inertia**

The anticipated maximum deflection at the center of the heat sink was calculated to be .0006 inches, which is quite small. The small deflection lead to the conclusion that the heat sink would not experience too much deflection under loading from the bolts, and therefore apply even contact pressure across the thermoelectric.

There was yet another issue to deal with before moving on. As the various components heat there is thermal expansion, which could change the loading on the bolts and thereby increase or decrease the contact pressure on the thermoelectrics. The problem is essentially statically indeterminate, because as the components grow they will elastically deform from the added load, which will both allow and limit the thermal expansion. To link the thermal expansion and elastic deformation the following equation was derived:

$$P = \frac{\alpha_{TE}\Delta T_{TE} L_{TE} + \alpha_{AL}\Delta T_{AL} L_{AL} - \alpha_{Bolt}\Delta T_{Bolt} L_{Bolt}}{\frac{L_{TE}}{A_{TE}E_{TE}} + \frac{L_{AL}}{A_{AL}E_{AL}} + \frac{L_{Bolt}}{nA_{Bolt}E_{Bolt}}}$$

**Equation 13: Resultant Load**

Ultimately, to relieve some pressure induced by the thermal expansion, bellvue spring washers were added below the bolts. They can absorb the deflection from the changing components [6].

**TEG Concept**

Based on the analysis the following concept was created using CAD software.

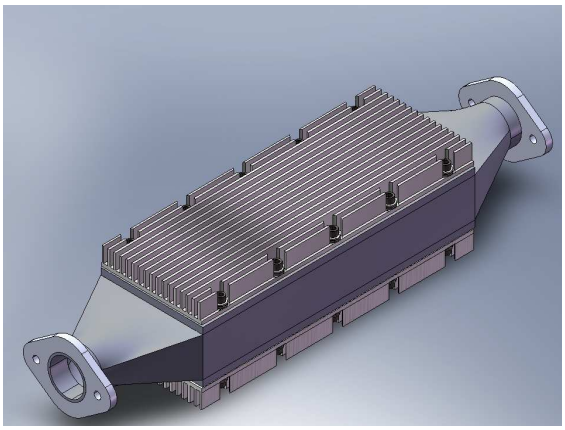

**Figure 7: Assembled 3-d Model**

The final concept is made up of 16 internal channels, two large heat sinks for cooling, and bellvue washers under the bolts to dissipate additional loading from thermal expansion.

**Construction**

Once all the parts and components have been analyzed to theoretically meet our needs, the parts were ordered and construction of the Thermal Electric Structure was underway. Inlays for the TEG on the top and bottom plate were the first machining task undertaken at the RIT machine shop. All but one of eight inlays was dimensioned to an accurate tolerance. In inlay 8 the CNC tool broke off slightly causing a defect on the overall smoothness of the inlay. This issue was addressed by inserting brass shims into the defected area to minimize any losses in heat transfer. Groves for fin placement were machined into the top and bottom aluminum plates on the RIT site. Accurate dimensions and tolerances were achieved. Both top and bottom plate bolt holes were milled and threaded with high precision and tolerance to achieve alignment with the extruded heat sink. The extruded heat sink was ordered from a

supplier. Machining of the heat sink included band sawing the heat sink in half, accurate removal of fins and precise placement of bolt holes. Removal of the fins was a daunting task that required great ingenuity in reducing fin vibration when undergoing the milling process. By clamping a plastic layer to the top of the fins, vibration was significantly reduced. The angle at which the fins were cut was vital in reducing fin and tool vibration. Once machining of the top and bottom plates was complete and all the fins had been cute to the appropriate width the groves were painted with silver thermal glue. The silver glue was thick and difficult to work with, water was applied to the solution making the gluing process far more tolerable. Fins were aligned into the bottom plate groves. The top plate was then aligned on the fins. The structure was placed in a vice with adequate pressure and left to set.

Plywood blower holders were designed and built to secure the leaf blowers in an appropriate angle to maximize the flow surface on the fins. Flow was simulated to be 45mph.

**Electrical Assembly Process:**

The TEGs are arranged as shown in Figure . Wiring the thermoelectric together are shown allows a large amount of freedom after the initial assembly because each row can either be placed in parallel or series with the surrounding rows to maximize the power to the load by impedance matching.

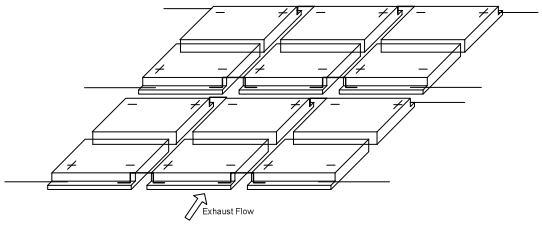


**Figure 8 - TEG Orientation and Wiring Scheme**

In order to maximize the space usage the thermoelectric wires were removed and then soldered in the correct direction to allow easy connections to the next thermoelectric in the row (REFER TO FIGURE 8). If the wires were simply bent to the next thermoelectric, the spacing between the rows would need to be increased significantly to allow for this bend radius.

The power control circuit shown in Figure was initially built in a prototyping, solderless breadboard to verify its functionality. The large majority of buck/boost chips, including the chosen chip that best matches the project requirements, are surface mount components. Since this is the case, an adapter board was necessary to allow for the integration of the surface mount chip with the rest of the (non-surface mount) circuitry. Once the circuit functionality is verified on the prototyping board, the components can then be soldered to a breadboard to create a more stable and robust circuit. The circuit is designed to take a large variety of input voltages, from approximately 20 to 60 V, and output approximately 14 V. This output level allows the TEGs to be connected to an automobile's electrical system and, more specifically, directly to the automobile's battery.

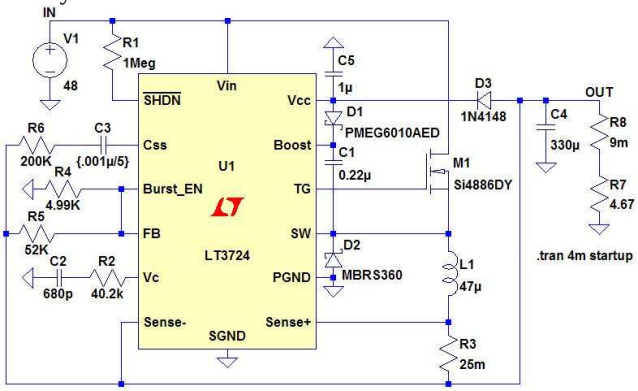


**Figure 9 - Power Control Unit Schematic [7]**

**Test plan**

The test plan has been created to verify the engineering specifications upon which the TEG concept design is based. All of the tests are performed under the standard test conditions, outlined earlier in this document. The specifications being verified are the maximum power generation, hot and cold side thermoelectric temperatures both up and down stream, inlet and outlet exhaust temperatures, the battery charging capability, and the pressure drop through the system.

A labview program has been developed to monitor the temperature readings on all eight thermocouples, the pressure sensor, inlet and outlet temperature sensors and exhaust mass flow rate. The exhaust testing unit will run on a ramp-up program to attain the desired ultimate testing temperature. Furthermore, as part of the test set-up, there are two blowers providing 45mph airflow over the two external finned heat sinks to replicate the wind created by a car traveling at 45mph. Each test takes approximately one hour to complete, not including the time needed to ramp the heater down and let the TEG unit cool. The maximum power reading is found by attaching the TEGs to a rheostat that is matched to the internal impedance of the TEG arrangement. Once the load is matched, the voltage across the rheostat will be measured and the relationship shown below will be used to determine the maximum output power.

$$P = \frac{V^2}{R}$$

**Equation 14: Max Output Power**

The ability to charge a battery can be determined by measuring the voltage across the battery. A slightly discharged battery, with a lower voltage, will be attached to the system and, after charging, an increase in the battery voltage, from approximately 11 V to 12.65 V, shall be verified. The voltage regulating system is expected to take any input voltage ranging from 4-60V and deliver a steady output of 13.5V and a charging current of 3A.

## III. RESULTS AND DISCUSSION

Ultimately the final, as tested version of the Thermoelectric Generator unit matched the final concept very closely, but there were some minor changes. The Permatex RTV 26B insulation specified in the bill of materials was replaced with Cotronics ceramic paper because of the much higher insulating properties associated with it. The Permatex RTV 26B thermal conductivity was approximately .3-.5 W/m-K while the Cotronics ceramic paper was on the order of 0.055 W/m-K. In the end the change was made in order to ensure that the thermal resistance was far greater around the thermoelectric modules so that less heat was able to bypass the thermoelectrics. Furthermore the Cotronics paper was added around the transitions and side walls to reduce heat loss through these areas to coincide with the assumptions made in the thermal analysis.

The results of testing have identified some issues in the design. The calculated resistance was lower than the results from testing suggest. Figure 10 illustrates the cold side temperatures experienced during testing under standard test conditions.

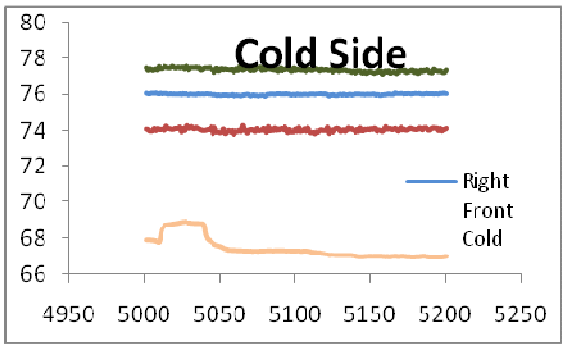


**Figure 10: Cold Side**

The discrepancy between the calculated temperatures and those tested come from a few key areas. First of all, there was an error in the model equating to a projected thermal resistance which was lower than the actual resistance. Secondly, the work input by the blowers on the air flowing over the fins increased the temperature of the air, there by becoming less able to remove heat through forced convection. Thirdly, the resistance to flow created by the close proximity of the fins causes a large quantity of the air to flow over the fins rather than through which reduces the effectiveness of forced convection. Lastly, the temperature of the testing room increases as the test progresses which in turn reduces the effectiveness of heat sinks.

Furthermore, the temperatures on the hot side did not reach the temperature anticipated from thermal modeling. Figure 11 shows the hot side temperatures obtained from testing under the standard test conditions outlined earlier in this document.

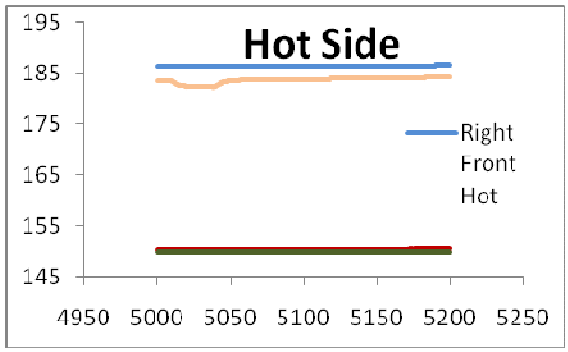


**Figure 11: Hot Side**

There are various reasons the TEG was not able to draw as much heat to the hot side as originally expected. There is inherent error when calculating convective coefficients which could have lead to some error. Also, it is possible that mixing issues exist within the exhaust gases themselves.

The resulting temperature differential across the thermoelectric module was lower than expected due to the unanticipated temperatures outlined in the paragraphs above. With a lower temperature differential the thermoelectric modules were only able to produce 40.4 Watts which is below the specified amount.

The battery charging circuitry was successfully completed. Numerous loads were attached to verify its functionality for a range of loads. For each load the output remained stable at the correct value of approximately 14 V. The circuit was also tested for a variety of input voltages. The output voltage remained constant for an input voltage swing from 20-60 V.

## IV. CONCLUSION

The Thermoelectric Generator designed throughout a 6 month period under project number P08441 met some, but not all, of the engineering specifications outlined early in the design phase. The maximum power generation specification of 65-100 Watts of electrical power was not met under the standard test conditions. Furthermore, the circuitry designed to charge the battery did not function as expected and ultimately did not meet the defined specification.

Overall, a series of issues lead to the overall inability to meet the critical specifications. To start, the cooling subsystem did not operate as efficiently as originally thought based on information supplied by the manufacturer.

The project was a great learning experience about the intricacies of trying to create power from thermoelectrics in a realistic environment.

Future improvements could greatly increase the power generation of the TEG unit. To begin, a less resistive heat sink could replace the current heat sink. Less thermal resistance would allow the finned heat sinks to cool more efficiently, increasing the temperature differential across the thermoelectric. Additionally, some sort of ducting system, that could efficiently direct the air over the fins, could cool the TEG unit better. Lastly, a cooling system could be designed to remove some of the heat from the air that the blower and rising room temperature adds.

## ACKNOWLEDGEMENTS

Dr. Robert Stevens

## REFERENCES


1. Melcor ThermElectric Coolers. 20 Feb. 2008 <http://www.melcor.com/tec.html>.
2. Introduction ThermoElectrics. 12 Aug. 2005 8 Feb. 2008 <http://thermoelectrics.com/intro.htm>
3. Incropera, F.P and Dewitt, D.P, 2007, *Fundamentals of Heat and Mass Transfer*, John Wiley & Sons, Danvers, MA, Chap. 8.
4. Fox, R.W, McDonald, A.T., and Pritchard, P.J., 2006, *Introduction to Fluid Mechanics*, John Wiley & Sons, Danvers, MA, Chap. 8.
5. Shigley, J.E, Mischke, C.R, and Budynas, R.G, 2004, *Mechanical Engineering Design*, McGraw-Hill, New York, NY, Chap. 8
6. Beer, F.P, Johnston, E.R, and DeWolf, J.T, 2002, *Mechanics of Materials*, McGraw-Hill, New York, NY, Chap. 2.
7. Linear Technology. 2007 14 Feb 2008 <www.linear.com>